

Electronic structure of metal/semiconductor interfaces from cathodoluminescence and soft X-ray photoemission spectroscopies

L.J. Brillson, I.M. Vitomirov, A. Raisanen, S. Chang, R.E. Viturro

Xerox Webster Research Center, 800 Phillips Road, W114-41D, Webster, NY 14580, USA

P.D. Kirchner, G.D. Pettit and J.M. Woodall

IBM T.J. Watson Research Center, Yorktown Heights, NY 10598, USA

Received 1 July 1992; accepted for publication 28 September 1992

The dependence of Schottky barrier formation on surface and interface preparation offers several broad avenues for understanding electronic structure and charge transfer at metal/semiconductor junctions. Interface cathodo- and photoluminescence measurements reveal that electrically active deep levels form at III–V and II–VI compound semiconductor surfaces and metal interfaces which depend on temperature-dependent surface stoichiometry and reconstruction, chemical interaction, as well as surface misorientation and bulk crystal quality. These interface states are discrete and occur at multiple gap energies which can account for observed band bending. Characteristic trends in such deep level emission with interface processing provide guides for optimizing interface electronic behavior. Correspondingly, photoemission and internal photoemission spectroscopy measurements indicate self-consistent changes in barrier heights which may be heterogeneous and attributable to interface chemical reactions observed on a monolayer scale. These results highlight the multiple roles of atomic-scale structure in forming macroscopic electronic properties of compound semiconductor/metal junctions.

1. Introduction

The understanding of interface electronic structure and charge transfer at metal/semiconductor interfaces has continued to challenge solid-state researchers for several decades [1,2]. Since localized charge states were first proposed to account for the relative insensitivity of semiconductor band bending to the bulk Fermi level difference between metal and semiconductor, researchers have proposed numerous physical models for such interface states. In general, these physical constructs aim to account for the Fermi-level “pinning” in a narrow energy range within the semiconductor band gap. More recently, considerable evidence has emerged to show that band bending can vary considerably for a given semiconductor – even for strongly “pinned” semiconductors such as GaAs [3–6]. Thus, significant changes in GaAs Schottky barrier height are seen

for (a) different metallizations on the same semiconductor surface, (b) different surface preparations for the same metal, and even (c) different methods of crystal growth for the same compound semiconductor.

The next section aims to show that substantial changes in barrier heights are achievable for metal interfaces with GaAs, both on a macroscopic and on an atomic scale. A number of factors appear to contribute to the interface electronic properties which are not intrinsic to the semiconductor or metal. Extrinsic features such as bulk crystal quality, interface chemical reaction and diffusion, as well as semiconductor surface morphology appear to have substantial effects on the range of Fermi-level stabilization energies. These large changes indicate that “pinning” models of Schottky barrier formation are inadequate to describe charge transfer at metal/semiconductor interfaces in general.

Section 3 provides evidence for additional contributions due to chemical processing. These include time- and temperature-dependent chemical reactions and suggest that contact inhomogeneities contribute significantly to macroscopic electronic measurements. These observations point to chemical composition and surface–interface bonding as major factors which cause large barrier height changes. Section 4 introduces the low-energy cathodoluminescence spectroscopy (CLS) technique and its applications to semiconductor interfaces. Combined with SXPS, the CLS technique provides a means to detect deep levels at metal/semiconductor interfaces as well as to correlate them with interface chemistry and band bending. Section 5 describes the application of the low-energy CLS technique to metal/GaAs (100) interfaces. Multiple deep levels are evident in the band gap which depend both on the starting clean surface and on the particular metal. Section 6 demonstrates the presence of a correlation between the deep levels observed via CLS and the Fermi-level position measured by SXPS. Included in this section is a summary of reported Fermi-level stabilization energies/band bending for Al on GaAs surface prepared in different ways. The large range of energies possible for the same metal on the same semiconductor emphasizes the importance of interface preparation and the need for models of Schottky barrier formation which do not presume “pinning” in a narrow energy range. Section 7 addresses the advantages of deep-level measurements at metal/semiconductor interfaces in practical models and analysis of Schottky barrier formation. Section 8 summarizes our results, namely that (i) discrete, process-dependent deep levels form a metal/semiconductor junctions, (ii) these interface-specific states correlate with the Fermi-level stabilization and (iii) chemical bonding and composition on an atomic scale play a major role in Schottky barrier formation.

2. Schottky barrier changes

In contrast to the Fermi-level “pinning” commonly assumed for Schottky barrier formation,

most semiconductors exhibit rather wide ranges of band bending with different metals. Even the GaAs/metal junction, which was believed to exhibit only a 0.2 eV variation near mid-gap, has now been found to yield a much wider range of band bending as a result of atomic-scale processing. Representative examples include: (a) the use of monolayer amounts of a reactive metal (e.g., Al) on a II–VI compound (e.g., CdS) to turn a rectifying contact into an injecting contact [3]; (b) the use of Si or Ge interlayers to alter the barrier heights of metal on GaAs over more than half the band gap [4]; (c) the use of orientation and annealing to modify the diode barriers of $\text{Sc}_x\text{Er}_{1-x}\text{As}/\text{GaAs}(100)$ lattice-matched interfaces by over 0.4 eV [5]. Such examples demonstrate that microscopic chemical structure affects macroscopic electronic structure and, indeed, large barrier height changes take place which depend on specifics of interface preparation such as growth method, metallization, and chemical interlayers.

Surface science techniques provide correlations between these barrier height changes and metal–semiconductor features on an atomic scale. Our group’s results have emphasized the role of both metallization and processing. Over the past few years, we have used soft X-ray photoemission spectroscopy (SXPS) in order to investigate the initial stages of Schottky barrier formation at metal/III–V compound semiconductor junctions. Because of the extremely high surface sensitivity of this technique, it is possible to follow and correlate the electronic and chemical structure of such interfaces as they are built up, monolayer by atomic monolayer. Our group has found a qualitative difference in the barrier formation of metals deposited on GaAs(100) surfaces grown by molecular beam epitaxy (MBE) versus ultra-high vacuum (UHV) cleaved GaAs(110) grown from the melt [6]. These MBE-grown (100) surfaces exhibit a wide (0.6–0.7 eV) range of Fermi-level (E_F) stabilization in the GaAs band gap versus 0.2–0.3 eV for the cleaved (100) surface. Indeed, it is possible to expand this range of E_F stabilization by processing the melt-grown (100) surfaces with the same procedures, e.g., thermal decapping of an As protective layer under UHV conditions, used for preparing the MBE GaAs

[7]. SXPS measurements also reveal an expanded range of band bending with variation in surface morphology [8,9]. The same metal – Al – on GaAs produces a 0.6 eV range of E_F stabilization as a function of surface misorientation direction and angle [8]. Here the band bending and interface state densities increase with increasing active atomic site density, inclusive of misoriented axis and angle [9].

3. Barrier and interface state changes with chemical processing

Macroscopic, internal photoemission measurements confirm the wide range of band bending revealed by SXPS measurements. This relatively

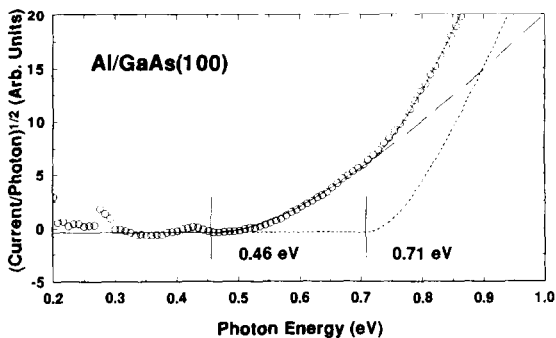
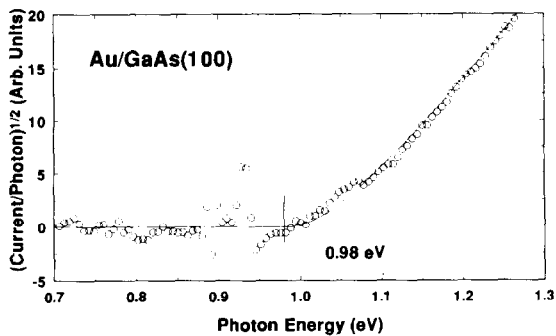


Fig. 1. Room-temperature internal photoemission spectra for Au (upper) and Al (lower) diodes with GaAs(100) surfaces. These two metals exhibit a pronounced difference in macroscopic electrical behavior. The Al diode behavior can be modeled by a two-barrier junction. See ref. [11].

well-defined barrier measurement exhibits clear differences between metals, e.g., 0.41 eV for Al, 0.93 eV for Cu, and 1.01 eV for Au following evaporation on GaAs(100) in UHV [10]. Significantly, the Al–GaAs(100) diodes exhibit internal photoemission features characteristic of multiple barriers. Fig. 1 shows the square-root dependence of internal photoemission current as a function of photon wavelength for Au(upper) versus Al(lower)–GaAs diodes [11]. In both cases, the barrier is determined by the onset of the quadratic fit. Not only do these two metals on GaAs differ substantially in terms of barrier height, but they differ in terms of homogeneity as well. The particular Al–GaAs diode shown exhibits features characteristic of two barriers, one at 0.46 eV and the other at 0.71 eV. In general, the Al–GaAs(100) diodes exhibit I – V characteristics corresponding to a low barrier of 0.37 ± 0.05 eV and a high barrier of 0.72 ± 0.04 eV. In contrast, the Au–GaAs(100) diodes are homogeneous, with a barrier of 1.01 ± 0.02 eV.

Annealing the Al diodes causes an increase in the low barrier and a growth of the low-barrier domains at the expense of the high-barrier domains. With time, these changes are observed even near room temperature. Furthermore, even the mechanical pressure associated with a wire contact to the diode overlayer induces electronic changes. These observations indicate the chemical activity of the interface and its major effect on electronic properties.

4. Low-energy cathodoluminescence spectroscopy at metal / semiconductor interfaces

We used a combination of CLS and SXPS to evaluate the correlation of interface states and band bending with chemical and structural conditions. The CLS technique is illustrated schematically in fig. 2 [12,13]. Here, incident electrons with energies of 0.5–5 keV produce a cascade of secondaries and electron–hole pairs within the top 100–1000 Å, which recombine via band-to-band and deep-level transitions. By varying the incident energy, one can preferentially enhance emission near the top surface. Unlike most sur-

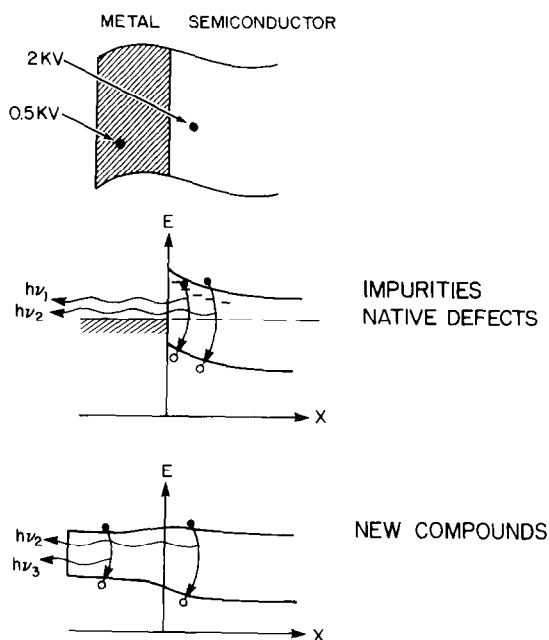


Fig. 2. Schematic illustration of low-energy cathodoluminescence spectroscopy (CLS) of metal/semiconductor interfaces. The incident electron beam can penetrate below the overlayer to the buried interface, creating electron-hole pairs which can recombine via band-to-band, deep-level, or new band structure transitions. See ref. [12].

face-sensitive techniques, CLS offers a means to probe electronic structure at a “buried” interface. CLS has already been successful in identifying (a) metal-induced interface states, i.e., different metals on InP(110) [14], (b) metal-induced state differences with crystal growth mode, i.e., Au on UHV-cleaved GaAs(110) grown from the melt versus Au on MBE-grown GaAs(100) [15], and (c) metal-induced states at vicinal surfaces, i.e., Al on stepped GaAs(100) versus misorientation angle and direction [8,9]. These and other results demonstrate that metals induce discrete gap states which depend on the semiconductor, the metal, the mode of crystal growth, and the surface morphology.

5. Interface states and band bending at reconstructed GaAs(100) / metal junctions

From the results presented thus far, the barrier changes with chemical processing appear to

be associated with either annealing or interface reactions. Annealing can deplete interface or subsurface As, it can anneal out native defects, and it is associated with the expanded range of barriers for both MBE and melt-grown GaAs. Interface reactions can “scavenge” excess As, they can produce interfacial layers with new dielectric properties, and they are evident for stepped surfaces, especially for reactive metals such as Al. It is therefore useful to examine the changes in interface state density and band bending as a function of surface processing in order to discriminate among these possible contributions. The different reconstructions of the GaAs(100) surface provide a good test bed for such studies, since it is possible to examine surfaces with the same reconstruction but different stoichiometries and vice versa.

We prepared different reconstructions of GaAs(100) using epitaxial films grown by MBE, moderately doped ($n = 1 \times 10^{17} \text{ cm}^{-3} \text{ Si}$), and capped in-situ with a thick ($\sim 5000 \text{ \AA}$) As layer to inhibit contamination. These specimens were shipped under vacuum from IBM to our laboratories at the Xerox Webster Research Center and to the University of Wisconsin’s Synchrotron Radiation Center, where they were thermally desorbed in UHV prior to analysis. Depending upon the temperature and rate of desorption as well as the ambient As backpressure within the UHV chamber, we obtained a variety of well-known reconstructions, including (1×1) , (2×4) - $c(2 \times 8)$, (4×2) - $c(8 \times 2)$, (4×6) , and a faceted surface reconstruction [16]. Surface stoichiometries based on SXPS As 3d ($h\nu = 100 \text{ eV}$) and Ga 3d ($h\nu = 80 \text{ eV}$) core-level intensities ranged from As/Ga = 1.5 to 0.7 for this set of reconstructions, respectively.

CLS spectra of the clean surfaces taken at $T = 175 \text{ K}$ exhibit only small differences between different reconstructions [17]. However, depth-dependent spectra obtained with different incident energies reveal substantial differences in spatial distribution of deep levels below the clean surfaces. For the clean $c(8 \times 2)$ (100) surface obtained at $T = 575^\circ\text{C}$, deep-level emission within the band gap is sensitive to probe depth, increasing with increasing surface sensitivity. For the

clean (1×1) (100) surface obtained at $T = 350^\circ\text{C}$, deep-level emission within the band gap is insensitive to probe depth, remaining constant as the energy of the incident electron probe was varied from 2.0 to 1.0 keV. These observations suggest that deep levels evident at the Ga-rich, $c(8 \times 2)$ surface are localized within the top few nanometers, whereas the deep levels at the As-rich, (1×1) surface are distributed more uniformly beneath the surface.

Metals on these reconstructed surfaces induce additional deep-level features which depend both on the particular metal as well as the particular reconstruction. As shown in fig. 3, a 10 Å deposit of Au on GaAs(100) (1×1) prepared at 350°C induces new deep-level emission at ~ 0.92 and ~ 1.17 eV, presumably involving transitions from the conduction band of this n-type material to acceptor levels at these energies below [17]. Nearly identical features are evident for Au on the GaAs(100) $c(8 \times 2)$ surface prepared at 520°C . With annealing at 300 K for 10 min, these features remain constant or increase slightly in am-

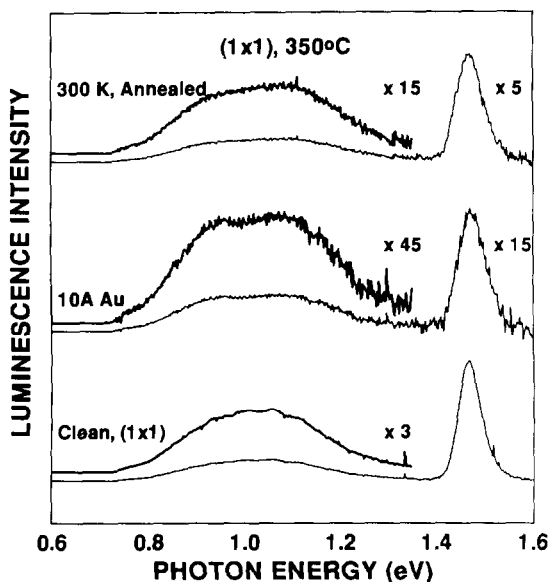


Fig. 3. CLS spectra at 1 keV and $T = 175$ K of the changes in deep-level emission at a clean GaAs(100) ($N_d = 7 \times 10^{16} \text{ cm}^{-3}$) (1×1) surface with 10 Å Au and subsequent annealing. Au induces new emission at ~ 0.92 and ~ 1.17 eV, which persists with subsequent annealing. See refs. [16,17].

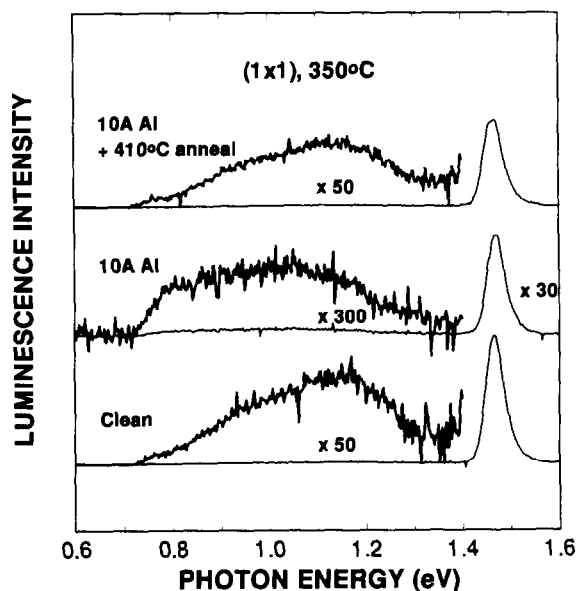


Fig. 4. CLS spectra at 1 keV and $T = 175$ K of the changes in deep-level emission at a clean GaAs(100) ($N_d = 7 \times 10^{16} \text{ cm}^{-3}$) (1×1) surface with 10 Å Al and subsequent annealing. Al induces new emission at ~ 0.8 eV, which is removed by subsequent annealing. See refs. [16,17].

plitude. Al on reconstructed GaAs(100) surfaces produces significantly different behavior. As shown in fig. 4, a 10 Å deposit of Al on GaAs(100) (1×1) prepared at 350°C induces new deep-level emission at ~ 0.8 eV and, to a lesser extent, at 0.95 eV [17]. Al on GaAs(100) reconstructed surfaces prepared at higher temperatures show monotonic changes in such deep-level features. Comparison of the (1×1) ($T = 350^\circ\text{C}$), $c(8 \times 2)$ ($T = 575^\circ\text{C}$), and (4×6) ($T = 620^\circ\text{C}$) (100) surfaces in fig. 5 reveals a steady decrease in the 0.8 eV peak feature, an increase in the 0.95 eV feature, and the emergence of a peak feature at 1.2 eV with increasing temperature and decreasing As surface composition. This monotonic change in relative amplitude of these three deep-level emission peak features suggests that the relative Ga-to-As near-surface composition, rather than the detailed surface reconstruction, has a dominant role in forming the deep-level features. Furthermore, annealing these interfaces at 410°C for 10 min effectively removes the metal-induced emission at 0.8 eV, in contrast to

the annealing behavior of the Au interfaces. Thus, the metallization and processing of the GaAs surface has a major effect upon the deep levels created at the metal/semiconductor interface. The nature of the deep-level transitions evident in these studies can be associated with CLS features uncovered under other interface conditions or with native defect levels reported for bulk GaAs. The 0.8 eV level can be associated with excess interface As observed for partially de-capped specimens [15]. The 0.95 eV level may be associated with the Fermi-level stabilization at 0.55–0.6 eV above the valence band edge observed for Al on vicinal GaAs(100) [8] or Al on p-type GaAs(100) [18]. The 1.05 eV emission appears to be bulk-related since it varies with growth technique. The 1.2 eV peak-emission feature may correspond either to a V_{Ga} acceptor or a Ga_{As} acceptor [19]. Perhaps most significantly, it is evident that the interface electronic states are discrete, deep within the band gap, and with energies and spatial distributions which can be

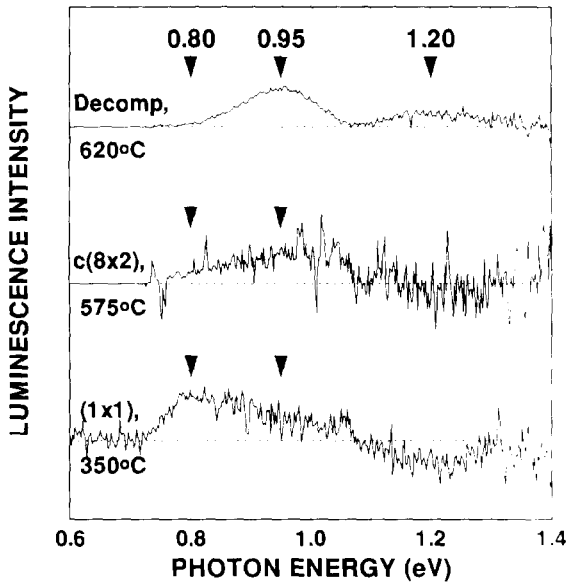


Fig. 5. CLS difference curves between GaAs(100) surfaces with and without 10 Å Al overlayers. With increasing temperature of surface preparation, the 0.8, 0.95, and 1.2 eV peak features change monotonically. These appear to depend primarily on near-surface Ga-to-As stoichiometry rather than surface reconstruction.

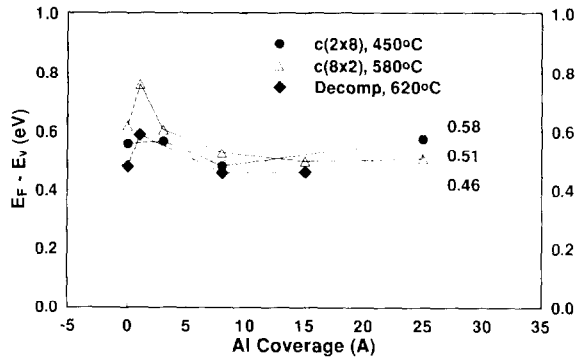


Fig. 6. Room-temperature Fermi-level movement as a function of Al deposition for three reconstructions of the GaAs(100) ($N_d = 7 \times 10^{16} \text{ cm}^{-3}$) surface. The Fermi level moves 0.12 eV closer to the valence band with increasing predeposition annealing temperature. See ref. [18].

related to specific surface composition, bulk crystal growth, or thermal treatment.

6. Deep-level correlation with Fermi-level stabilization

The interface states detected via CLS appear to influence the Fermi-level stabilization of the metal/semiconductor interface. Fig. 6 illustrates how the Fermi-level position above the valence band moves as a function of Al deposition on the clean GaAs(100) surface for three different reconstructions – (2 × 4) at $T = 450^\circ\text{C}$, c(2 × 8) at $T = 580^\circ\text{C}$, and a faceted (decomposed) surface at $T = 620^\circ\text{C}$. With increasing temperature, the Fermi level for the metallized surface stabilizes closer to the valence band. Depending upon the method of establishing the valence-band edge from an extrapolation of the SXPS valence-band spectra, such differences in E_F stabilization correspond to band-bending changes of between 0.1 and 0.2 eV. These E_F stabilization energies are consistent with the increasing emission strength of the lowest-lying deep levels with increasing temperature.

These Fermi-level (E_F) stabilization energies lie within a rather extended range of positions obtained by various researchers for Al on GaAs. Indeed, fig. 7 shows that, for the same metal on

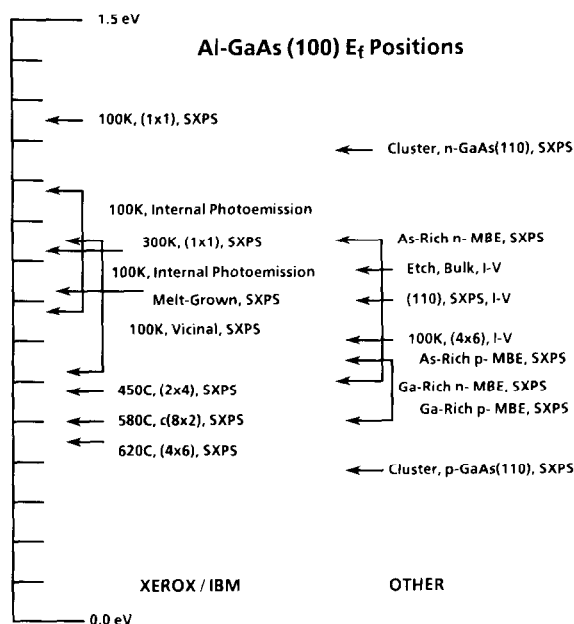


Fig. 7. Fermi-level stabilization energies for Al/GaAs interfaces as a function of growth and processing. Xerox/IBM results appear on the left, other groups' results on the right. References and energy values appear in the text for each arrow. The wide variation in energy emphasizes the importance of surface and interface preparation and the controllability of the Schottky barrier formation.

the same semiconductor, this range can extend from 0.46 to 1.2 eV above the valence-band edge, depending upon the composition, growth method, and doping. These E_F stabilization energies for Al on the three GaAs(100) reconstructed surfaces described in fig. 5 appear at the lowest energies (0.46–0.58 eV) of those reported by the Xerox/IBM group [17]. We measured higher values corresponding to the vicinal surfaces in refs. [8,9] (0.64–0.96 eV), the melt-grown and As-decapped surface in ref. [7] (0.81 eV), the (As-rich) decapped surfaces, measured by internal photoemission in fig. 1 (0.78–1.06 eV) [11], and the (1 × 1) As-decapped surfaces measured by SXPS (0.93–1.25 eV) [6]. With the exception of our group's 1.2 eV data point for Al on GaAs(100) (1 × 1) obtained by SXPS at 100 K [6], a range of Al–GaAs E_F stabilization from 0.5 to 1.0 eV above the valence band has been confirmed by

the photoemission and current–voltage measurements of other groups. These measurements include “inert” surfaces prepared by deposition of metal clusters using Xe buffer layers on n-type (1.17 eV) and p-type (0.38 eV) GaAs [22], As-rich, n-type (0.93 eV) and p-type (0.6 eV) surfaces, Ga-rich, n-type (0.6–0.7 eV) and p-type (0.5 eV) surfaces [20,21], a (4 × 6) surface measured by I – V (0.7 eV) [21], a bulk-grown, etched surface (0.85 eV) [4], and, for comparison, a cleaved (110), bulk-grown surface (0.8 eV) [23]. Observations of both our group and others indicate that the higher-lying stabilization energies correspond to more As-rich surface conditions. Experiments are in progress to evaluate the electronic structure associated with such process conditions. In general, the wide range of E_F positions for Al/GaAs interfaces demonstrates the importance of extrinsic effects such as atomic composition and morphology. Furthermore, the changes in interface state distributions with surface preparation evident in the CLS features shown in figs. 3–5 suggest the importance of surface chemical composition and its sensitivity to atomic-scale processing in determining the band bending of the metal/semiconductor interface.

7. Deep-level / chemistry basis for Schottky barrier formation

The changes in deep-level interface states in figs. 3–5 and the changes in Schottky barrier formation shown in figs. 6 and 7 demonstrate the importance of surface preparation in Schottky barrier formation. The influence of chemistry, surface morphology, and even bulk crystal growth on the subsequent interface properties indicates that several physical phenomena can contribute to interface state formation. This is consistent with the generally extended rather than abrupt nature of the metal–semiconductor contact [1]. For interfaces with reacted/interdiffused regions and/or point and extended defects and impurities, the strength and nature of these chemical interactions dominate the junction electronic properties [1,24]. The wide range of band bending evident even for GaAs junctions has a serious

implication for models of Schottky barrier formation. Practical models of Schottky barrier formation should, at a minimum, provide reasonable agreement with experiment measurements of well-characterized junctions. The wide range of band bending reported by several groups is not adequately described by "pinning" models, extrinsic [25] or intrinsic [26]. In addition, a useful model of Schottky barrier formation should predict as well as rationalize barrier behavior, providing tests of interface band bending versus electronic structure. Ideally such a model would predict macroscopic electronic properties on the basis of features measurable on an atomic scale. Alternatively, atomic-scale features measured in-situ during semiconductor growth and processing might provide diagnostics for macroscopic devices prior to completing their fabrication.

The correlation between deep levels observed via CLS and the changes in GaAs (and other semiconductor) band bending suggests a useful basis for describing and perhaps predicting band-bending properties. In this deep level/chemistry picture, a wide range of band bending is possible, depending on the presence or absence of deep levels. The deep levels can arise from a variety of defects, impurities, complexes, precipitates, dislocations, or other near-surface chemical features. Depending upon the energies and densities of these deep levels, the E_F stabilizes at different positions as deviations from a simple Schottky model of charge transfer. Such a physical picture is in contrast to a "defect" model, for example, where a particular native defect (i.e., EL2) leads to a "pinning" for all adsorbates within the narrow range of energy levels of this defect [25]. Extraction of energies and densities of all deep levels, coupled with a self-consistent electrostatic analysis (for example, ref. [27]) could then provide a means to predict band bending from atomic-scale electronic measurements. Such an advance requires new sub-gap, transient optical response measurements, optical detection and/or excitation of states throughout the band gap, and a theory describing such optical phenomena in terms of state densities and cross sections for charge capture and release in the near-surface region. Such deep-level measure-

ments and optical emission theory are not yet available.

8. Conclusions

The CLS and SXPS results presented here demonstrate that discrete deep levels are present in the GaAs band gap which are sensitive to the specifics of semiconductor growth, interface chemistry, and subsequent processing. Likewise, numerous studies indicate that band bending at GaAs/metal interfaces can vary over a substantial range and is dependent on the detailed interface chemical conditions. Indeed a correlation is evident between the band bending observed via SXPS and the deep-level energies plus emission intensities extracted from CLS. This correlation suggests that deep levels controlled by interface preparation may provide a useful basis for understanding and perhaps predicting Schottky barrier properties.

Acknowledgements

Partial support by the Office of Naval Research under contract #N00014-91-C-0037 is gratefully acknowledged. Soft X-ray photoemission spectroscopy was performed at the University of Wisconsin's Synchrotron Radiation Center, which is supported by the National Science Foundation.

References

- [1] L.J. Brillson, *Surf. Sci. Rep.* 2 (1982) 123.
- [2] E.H. Rhoderick and R.H. Williams, *Metal-Semiconductor Contacts*, 2nd ed. (Clarendon, Oxford, 1988).
- [3] C.F. Brucker and L.J. Brillson, *Appl. Phys. Lett.* 39 (1981) 67.
- [4] J.R. Waldrop and R.W. Grant, *Appl. Phys. Lett.* 50 (1987) 250;
R.W. Grant and J.R. Waldrop, *J. Vac. Sci. Technol. B* 5 (1987) 1015.
- [5] C.J. Palmström, T.L. Cheeks, H.L. Gilchrist, J.G. Zhu, C.B. Carter and R.E. Nahory, in: *Electronic, Optical, and Device Properties of Layered Structures*, Eds. J.R. Hayes, M.S. Hysbertson and E.R. Weber (Materials Research Society, Pittsburgh, PA, 1990) p. 63.

- [6] R.E. Viturro, J.L. Shaw, C. Mailhot, L.J. Brillson, N. Tache, J. McKinley, G. Margaritondo, J.M. Woodall, P.D. Kirchner, G.D. Pettit and S.J. Wright, *Appl. Phys. Lett.* 52 (1988) 2052;
R.E. Viturro, J.L. Shaw, L.J. Brillson, J.M. Woodall, P.D. Kirchner, G.D. Pettit and S.J. Wright, *J. Vac. Sci. Technol. B* 6 (1988) 1397.
- [7] S. Chang, I. Vitomirov, L.J. Brillson, D.S. Rioux, P.D. Kirchner, D. Pettit and J.M. Woodall, *J. Vac. Sci. Technol. B* 9 (1991) 2129.
- [8] S. Chang, L.J. Brillson, Y.J. Kime, D.S. Rioux, P.D. Kirchner, D. Pettit and J.M. Woodall, *Phys. Rev. Lett.* 64 (1990) 2551; *J. Vac. Sci. Technol. B* 8 (1990) 1008.
- [9] S. Chang, L.J. Brillson, D.S. Rioux, P.D. Kirchner, D. Pettit and J.M. Woodall, *Phys. Rev. B* 44 (1991) 1391.
- [10] S. Chang, R.E. Viturro and L.J. Brillson, *J. Vac. Sci. Technol. A* 8 (1990) 3803.
- [11] S. Chang, A.D. Raisanen, L.J. Brillson, J.L. Shaw, P.D. Kirchner, G.D. Pettit and J.M. Woodall, *J. Vac. Sci. Technol.*, in press.
- [12] L.J. Brillson, H.W. Richter, M.L. Slade, B.A. Weinstein and Y. Shapira, *J. Vac. Sci. Technol. A* 3 (1985) 1011.
- [13] L.J. Brillson and R.E. Viturro, *Scanning Electron Microsc.* 2 (1988) 789.
- [14] R.E. Viturro, M.L. Slade and L.J. Brillson, *Phys. Rev. Lett.* 57 (1986) 487.
- [15] R.E. Viturro, M.L. Slade and L.J. Brillson, *J. Vac. Sci. Technol. A* 5 (1987) 1516.
- [16] I.M. Vitomirov, A.D. Raisanen, L.J. Brillson, P.D. Kirchner, G.D. Pettit and J.M. Woodall, *J. Vac. Sci. Technol.*, in press.
- [17] I.M. Vitomirov, A.D. Raisanen, R.E. Viturro, S. Chang, L.J. Brillson, P.D. Kirchner, G.D. Pettit and J.M. Woodall, *J. Vac. Sci. Technol.*, in press.
- [18] I.M. Vitomirov, A.D. Raisanen, L.J. Brillson, P.D. Kirchner, G.D. Pettit and J.M. Woodall, *J. Electron. Mater.*, submitted.
- [19] J.F. Wager and J.A. van Vechten, *Phys. Rev. B* 35 (1987) 2330.
- [20] S.P. Svensson, G. Landgren and T.G. Andersson, *J. Appl. Phys.* 54 (1983) 4474.
- [21] S.P. Svensson, J. Kanski, T.G. Andersson and P.O. Nilsson, *J. Vac. Sci. Technol. B* 2 (1984) 235.
- [22] G.D. Waddill, I.M. Vitomirov, C.M. Aldao, S.G. Andersson, C. Capasso, J.H. Weaver and Z. Lilienthal-Weber, *Phys. Rev. B* 41 (1990) 5293.
- [23] N. Newman, W.E. Spicer, T. Kendelewicz and I. Lindau, *J. Vac. Sci. Technol. B* 4 (1986) 931.
- [24] L.J. Brillson, in: *Handbook on Semiconductors*, Vol. 1, 2nd ed. (North-Holland, Amsterdam, 1992) ch. 7.
- [25] W.E. Spicer, Z. Lilienthal-Weber, E. Weber, N. Newman, T. Kendelewicz, R. Cao, C. McCants, P. Mahowald and I. Landau, *J. Vac. Sci. Technol. B* 6 (1988) 1245.
- [26] J. Tersoff, *Phys. Rev. B* 32 (1985) 6968;
V. Heine, *Phys. Rev.* 138 (1965) A1689.
- [27] C.B. Duke and C. Mailhot, *J. Vac. Sci. Technol. B* 3 (1985) 170.